厚生科学研究費補助金研究報告書

平成10年度　高度先端医療研究事業

人工血液

遺伝子導入とサイトカインによる巨核球系白血病の分化による血小板の生成の研究（H10－血液－002）

申請者　畠　清彦

自治医科大学血液学

別紙2

厚生科学研究費補助金（高度先端医療研究事業）

総括研究報告書

遺伝子導入とサイトカインによる巨核球系白血病の分化による血小板の生成の研究

主任研究者　　畠　清彦　　自治医科大学　血液学

研究要旨　　川崎病での血小板増加はM-CSF,IL-6によりおこっていること、また白血病細胞株においてbcl-XLを遺伝子導入すると巨核球系へと分化すること、HIV由来vprは核数の制御に重要であり、遺伝子導入細胞の制御に重要である新規蛋白として内皮細胞由来IL-8,その分泌を担当する内皮細胞が細胞死の機構に重要であることが明らかになった。

分担研究者　照井　康仁
自治医科大学血液学
講師

A.研究目的

血小板の分化、機能を刺激する至適なサイトカインと巨核球への分化を誘導する遺伝子、転写因子GATAを用いて巨核球系白血病を分化させ、血小板の生成を計画する研究を行う。緊急に出血傾向を伴う患者さんの手術に対して出血の防止に作用できるものを開発する。

B.研究方法

白血病細胞株K562細胞にアポトーシスを制御する遺伝子を強制発現させることによって、巨核球系に分化する遺伝子を検索した。また骨髄異形成症候群患者由来の細胞を各種のサイトカインを添加して培養し、株細胞の樹立を試みた。また応用される白血病細胞の増殖停止及び細胞死をおこして制御するために白血病に対するアポトーシス誘導因子を解析した。白血病株細胞HL-60を分化誘導因子とともに培養し、その上清から高速液体クロマトグラフィを用いて精製した。精製した蛋白の構造を決定し、作用機序を解析した。

C.研究結果

白血病細胞のうち、アポトーシスに関連した遺伝子として、bcl-XLを強制発現させると巨核球系へ分化することがわかった。樹立した白血病細胞株では、インターロイキン3,GM-CSFに反応して増殖し、トロンボポエチンにも反応することがわかった。分化を誘導して血小板構造物が出現するかどうか検討する。新しいアポトーシス誘導因子として内皮細胞由来インターロイキン８がみいだされ、内皮細胞がアポトーシスに関与していることを報告した。

D.考察

bcl－XLが巨核球系への分化を決定する因子のひとつであることが判明したが、最近他に転写因子GATAファミリーやトロンボポエチン受容体も分化決定に重要と考察された。新しく樹立された細胞株からは今後転写因子GATAファミリーやトロンボポエチン受容体遺伝子を導入し発現をさせて血小板まで出現するかどうかを検討する。アポトーシス誘導遺伝子を使用して、白血病細胞の死や分裂増殖停

止に有用かを検討が必要である。

E.結論

巨核球系への分化に重要な遺伝子 bcl-XL を見い出し、アポトーシス誘導因子を新たに見い出した。これらは巨核球／血小板系への分化と細胞増殖の制御に重要と考えられ、今後の発展性が高い。

F.研究発表

1．論文発表

Terui Y, Tomizuka H, Ohtsuki T, Uwai M, Mori M, Hatake K.: Activated endothelial cells induces apoptosis in leukemic cells by endothelial interleukin-8. Blood, 92:2672-2680, 1998.

Terui Y, Tomizuka H, Uwai M, Mori M, Hatake K.: Identification of a novel apoptosis-inducing factor derived from leukemic cells: Endothelial interleukin-8, but not monocyte-derived, induces apoptosisin leukemic cells.
Biochem Biophy Res Comm
243:407-411, 1998.

Terui Y, Furukawa Y, Hatake K, Kitagawa S, Miura Y.:Bcl-X Is a Regulatory Factor of Apoptosis and Differentiation in Megakaryocytic Lineage Cells. Exp Hematol, 26:236-244, 1998.

2．学会発表

第 60 回日本血液学会総会
1998 年 3 月 25 日～27 日
白血病細胞に対する新規アポトーシス誘導因子の in vivo における効果

第 55 回日本癌学会総会
1996 年 10 月 10～12 日
K562 細胞の分化誘導時における bcl-x の役割

第 56 回日本癌学会総会　1997 年 9 月 27 日
白血病細胞由来の新しいアポトーシス誘導因子ー抗癌作用としての可能性

第 57 回日本癌学会総会
1998 年 9 月 30 日～10 月 2 日
内皮細胞による新しいアポトーシス誘導系：内皮細胞由来 IL-8 の関与

Sapporo Cancer Seminar Foundation
1998 年 7 月 6 日～8 日
Endothelial cells in a novel apoptosis system: Anti-tumor effect of IL-8 derived from endothelial cells.

ISEH' 1998 年 8 月 1 日～5 日
Anti-Tumor Effect of Endothelial IL-8 by Induction of an Apoptosis:Participation of Endothelial Cells in a Novel Apoptosis system.

別紙2

厚生科学研究費補助金（高度先端医療研究事業）

総括研究報告書

遺伝子導入とサイトカインによる巨核球系白血病の分化による血小板の生成の研究

主任研究者　畠　清彦　自治医科大学　血液学

研究要旨　川崎病での血小板増加はM-CSF,IL-6によりおこっていること、また白血病細胞株においてbcl-XLを遺伝子導入すると巨核球系へと分化すること、HIV由来vprは核数の制御に重要であり、遺伝子導入細胞の制御に重要である新規蛋白として内皮細胞由来IL-8,その分泌を担当する内皮細胞が細胞死の機構に重要であることが明らかになった。

分担研究者　大月　哲也
自治医科大学血液学
講師

A.研究目的

血小板の分化、機能を刺激する至適なサイトカインと巨核球への分化を誘導する遺伝子、転写因子GATAを用いて巨核球系白血病を分化させ、血小板の生成を計画する研究を行う。緊急に出血傾向を伴う患者さんの手術に対して出血の防止に作用できるものを開発する。

B.研究方法

白血病細胞の分化に作用する遺伝子を、細胞株にall-trans retinoic acidを作用させ、発現増強する遺伝子をクローニングした。重症貧血のうちのひとつである、Fanconi貧血の遺伝子異常を研究した。特に病態について研究した。

C.研究結果

Src-like adapter protein(SLAP)がクローニングされたので、全長配列を決定し、報告した。またFanconi貧血の遺伝子異常についてはNF-kBファミリーのひとつである転写因子が結合していることがわかり、投稿準備中である。

D.考察

Fanconi貧血は重症であり、治療の開発、特に遺伝子治療の標的となっている疾患である。アポトーシスの異常も認められており、血球減少のメカニズムとしても解析が望まれる。

別紙2

厚生科学研究費補助金（高度先端医療研究事業）

総括研究報告書

遺伝子導入とサイトカインによる巨核球系白血病の分化による血小板の生成の研究

主任研究者　畠　清彦　自治医科大学　血液学

研究要旨　川崎病での血小板増加はM-CSF,IL-6によりおこっていること、また白血病細胞株においてbcl-XLを遺伝子導入すると巨核球系へと分化すること、HIV由来vprは核数の制御に重要であり、遺伝子導入細胞の制御に重要である新規蛋白として内皮細胞由来IL-8,その分泌を担当する内皮細胞が細胞死の機構に重要であることが明らかになった。

分担研究者　冨塚　浩
自治医科大学血液学
講師

A.研究目的

血小板の分化、機能を刺激する至適なサイトカインと巨核球への分化を誘導する遺伝子、転写因子GATAを用いて巨核球系白血病を分化させ、血小板の生成を計画する研究を行う。緊急に出血傾向を伴う患者さんの手術に対して出血の防止に作用できるものを開発する。

B.研究方法

血液幹細胞の1分画であるCD34陽性細胞においてアポトーシスを制御する遺伝子bcl-2ファミリー、Fas抗原(CD95)を検索した。方法としてコロニー形成細胞をつりあげて、PCRを用いて遺伝子発現を検討した。急性前骨髄性白血病に対するアポトーシス誘導因子を解析した。CD95、bcl-2ファミリーを検討した。

C.研究結果

アポトーシスに関連した遺伝子として、急性前骨髄性白血病では、CD95は分化誘導療法の有効例では先立って発現増強が認められた。また血液幹細胞ではCD95が発現が低く、アポトーシスに陥らないような機序があると考えられた。

D.考察

血液幹細胞のうちCD34陽性細胞ではCD95がTNFa,Interferon g系が抑制的に作用して、アポトーシスを誘導して、幹細胞の数や増殖を調節している。アポトーシスではさらに血管内皮細胞と幹細胞との相互作用が重要であることが認められたので、今後細胞間または、誘導因子と幹細胞との影響を検討する必要がある。

E.結論

急性前骨髄性白血病ではCD95が発現増強されると、分化誘導療法に対して有効であり、有効性の予測でも有用であることを示した。コロニー形成細胞ではbcl-2ファミリーがアポトーシス阻止に作用していると考えられている。

F.研究発表

1.論文発表

Tomizuka H, Hatake K, et al.: CD95 predicts responsiveness to tretinoin in acute promyelocytic

leukemia.
Int J Mol Med 1:207-211, 1998.
Hatake K, Tomizuka H, Ikeda M, Terui Y, Miura Y.: Apoptosis-gene expression in hematopoietic system: Normal and pathological conditions.
Int J Mol Med 1:121-9, 1998.
Terui Y, Tomizuka H, Ohtsuki T, Uwai M, Mori M, Hatake K.: Activated endothelial cells induces apoptosis in leukemic cells by endothelial interleukin-8.
Blood 92:2672-2680, 1998.
Terui Y, Tomizuka H, Uwai M, Mori M, Hatake K.: Identification of a novel apoptosis-inducing factor derived from leukemic cells.: Endothelial interleukin-8, but not monocyte-derived, induces apoptosis in leukemic cells.
Biochem Biophy Res Comm 243:407-411, 1998.
Igarashi H, Hatake K, Tomizuka H,: High serum level of macrophage colony-stumlating factor and granulocytic colony-stimulating factor in Kawasaki disease.
Brit J Haematol, 1999 in press.

別紙2

厚生科学研究費補助金（高度先端医療研究事業）

総括研究報告書

遺伝子導入とサイトカインによる巨核球系白血病の分化による血小板の生成の研究

主任研究者　畠　清彦　自治医科大学　血液学

研究要旨　川崎病での血小板増加はM-CSF,IL-6によりおこっていること、また白血病細胞株においてbcl-XLを遺伝子導入すると巨核球系へと分化すること、HIV由来vprは核数の制御に重要であり、遺伝子導入細胞の制御に重要である新規蛋白として内皮細胞由来IL-8,その分泌を担当する内皮細胞が細胞死の機構に重要であることが明らかになった。

分担研究者　上井　雅哉
自治医科大学血液学
大学院生

A.研究目的

血小板の分化、機能を刺激する至適なサイトカインと巨核球への分化を誘導する遺伝子、転写因子GATAを用いて巨核球系白血病を分化させ、血小板の生成を計画する研究を行う。緊急に出血傾向を伴う患者さんの手術に対して出血の防止に作用できるものを開発する。

B.研究方法

応用される白血病細胞の増殖停止及び細胞死をおこして制御するために白血病に対するアポトーシス誘導因子を解析した。白血病株細胞HL-60を分化誘導因子とともに培養し、その上清から高速液体クロマトグラフィを用いて精製した。精製した蛋白の構造を決定し、作用機序を解析した。

C.研究結果

白血新しいアポトーシス誘導因子として補体ファクター蛋白Bbがみいだされ、補体系蛋白がアポトーシスに関与していることを報告した。

D.考察

アポトーシス誘導遺伝子を使用して、白血病細胞の死や分裂増殖停止に有用かを検討が必要である。補体系はこれまでにアポトーシスに関連するという報告はなく、新しい発見であり、発展性がある。

E.結論

これらは巨核球／血小板系への分化と細胞増殖の制御に重要と考えられ、今後の発展性が高い。

F.研究発表

1.論文発表

Terui Y, Tomizuka H, Ohtsuki T, Uwai M, Mori M, Hatake K.: Activated endothelial cells induces apoptosis in leukemic cells by endothelial interleukin-8. Blood 92:2672-2680, 1998.

Terui Y, Tomizuka H, Uwai M, Mori M, Hatake K.: Identification of a novel apoptosis-inducing factor derived from leukemic cells: Endothelial interleukin-8, but not monocyte-derived, induces apoptosis in leukemic cells. Biochem Biophy Res Comm 243:407-411, 1998.

2.学会発表

第60回日本血液学会総会

1998年3月25日～27日

新しい白血病細胞由来アポトーシス誘導因子；補体B

Sapporo Cancer Seminar Foundation

1998年7月6日～8日

Purification of Apoptosis-Inducing Factor to Homogeneity of a Human Complement Factor B-Derived Fragment.

別紙2

厚生科学研究費補助金（高度先端医療研究事業）

総括研究報告書

遺伝子導入とサイトカインによる巨核球系白血病の分化による血小板の生成の研究

主任研究者　　畠　清彦　　自治医科大学　血液学

研究要旨　　川崎病での血小板増加はM-CSF,IL-6によりおこっていること、また白血病細胞株においてbcl-XLを遺伝子導入すると巨核球系へと分化すること、HIV由来vprは核数の制御に重要であり、遺伝子導入細胞の制御に重要である新規蛋白として内皮細胞由来IL-8,その分泌を担当する内皮細胞が細胞死の機構に重要であることが明らかになった。

分担研究者　森　政樹
自治医科大学血液学
大学院生

A.研究目的

血小板の分化、機能を刺激する至適なサイトカインと巨核球への分化を誘導する遺伝子、転写因子GATAを用いて巨核球系白血病を分化させ、血小板の生成を計画する研究を行う。緊急に出血傾向を伴う患者さんの手術に対して出血の防止に作用できるものを開発する。

B.研究方法

応用される白血病細胞の増殖停止及び細胞死をおこして制御するために白血病に対するアポトーシス誘導因子を解析した。白血病株細胞HL-60を分化誘導因子とともに培養し、その上清から高速液体クロマトグラフィを用いて精製した。精製した蛋白の構造を決定し、作用機序を解析した。

C.研究結果

白血新しいアポトーシス誘導因子としてβ2-microglobulinがみいだされ、T細胞とHLA分子がアポトーシスに関与していることを報告した。現在投稿し、revised versionのための追加実験を行っている。

D.考察

アポトーシス誘導遺伝子を使用して、白血病細胞の死や分裂増殖停止に有用かを検討が必要である。またHLA分子、β2-microglubulinとサイトメガロウィルス感染症との関連、移植後のGVHDの機序にも重要と考えられる。

E.結論

これらは巨核球／血小板系への分化と細胞増殖の制御に重要と考えられ、今後の発展性が高い。

F.研究発表

1.論文発表

Terui Y, Tomizuka H, Ohtsuki T, Uwai M, Mori M, Hatake K.: Activated endothelial cells induces apoptosis in leukemic cells by endothelial interleukin-8. Blood 92:2672-2680, 1998.

Terui Y, Tomizuka H, Uwai M, Mori M, Hatake K.: Identification of a novel apoptosis-inducing factor derived from leukemic cells: Endothelial

interleukin-8, but not monocyte-derived, induces apoptosis in leukemic cells.
Biochem Biophy Res Comm 243:407-411,1998.

2.学会発表

第40回日本臨床血液学会
1998年11月11日～13日
白血病細胞株に対するβ2ミクログロブリンのアポトーシス誘導効果

第60回日本血液学会総会
1998年3月25日～27日
白血病細胞株に対するβ2ミクログロブリンのアポトーシス誘導因子

第57回日本癌学会総会
1998年9月30日～10月2日
白血病細胞株に対するβ2ミクログロブリン誘導アポトーシスの検討

Sapporo Cancer Seminar Foundation
1998年7月6日～8日
BETA-2 Microglobulin-Induced Apoptosis in Human Leukemic Cell Lines.

ISEH' 1998年8月1日～5日
A Novel Apoptosis-Inducible Effect of BETA-2 Microglobulin in Human Cell Lines.

THE JOURNAL OF BIOLOGICAL CHEMISTRY
© 1998 by The American Society for Biochemistry and Molecular Biology, Inc.

Vol. 273, No. 41, Issue of October 9, pp. 26779–26789, 1998
Printed in U.S.A.

Single Glycosyltransferase, Core 2 β1→6-*N*-acetylglucosaminyltransferase, Regulates Cell Surface Sialyl-Le^x Expression Level in Human Pre-B Lymphocytic Leukemia Cell Line KM3 Treated with Phorbolester*

(Received for publication, January 5, 1998, and in revised form, July 21, 1998)

Mitsuru Nakamura‡§, Takashi Kudo¶, Hisashi Narimatsu¶, Yusuke Furukawa‡, Jiro Kikuchi‡‖, Shinji Asakura**, Wei Yang**, Satsuki Iwase‡ ‡‡, Kiyohiko Hatake§§, and Yasusada Miura‡§§

*From the ‡Division of Hemopoiesis, and **Division of Hemostasis and Thrombosis, Research Institute of Hematology, and §§Department of Hematology, Jichi Medical School, Minamikawachi, Tochigi 329-04, Japan, the ¶Division of Cell Biology, Institute of Life Science, Soka University, 1-236 Tangi, Hachioji, Tokyo 192, Japan, ‖Katsuta Research Laboratory, Hitachi Koki Co., Ltd., Hitachinaka, Ibaraki 312, Japan, and the ‡‡Department of Internal Medicine, Jikei University School of Medicine, Tokyo 105, Japan*

Sialyl-Le^x (sLe^x) antigen expression recognized by KM93 monoclonal antibody was significantly down-regulated during differentiation induced by 12-*O*-tetradecanoylphorbol-13-acetate (TPA) in human pre-B lymphocytic leukemia cell line KM3. The sLe^x determinants were almost exclusively expressed on *O*-linked oligosaccharide chains of an *O*-glycosylated 150-kDa glycoprotein (gp150). A low shear force cell adhesion assay showed that TPA treatment significantly inhibited E-selectin-mediated cell adhesion. Transcript and/or enzyme activity levels of α1→3-fucosyltransferase, α2→3-sialyltransferase, β1→4-galactosyltransferase, and elongation β1→3-*N*-acetylglucosaminyltransferase did not correlate with sLe^x expression levels. However, transcript and enzyme activity levels of core 2 GlcNAc-transferase (C2GnT) were significantly down-regulated during TPA treatment. Following transfection and constitutive expression of full-length exogenous C2GnT transcript, C2GnT enzyme activities were maintained at high levels even after TPA treatment and down-regulation of cell surface sLe^x antigen expression by TPA was completely abolished. Furthermore, in the transfected cells, the KM93 reactivity of gp150 was not reduced by TPA treatment, and the inhibition of cell adhesion by TPA was also blocked. These results suggest that sLe^x expression is critically regulated by a single glycosyltransferase, C2GnT, during differentiation of KM3 cells.

Sialyl-Le^x (sLe^x)[1] and sialyl-Le^a structures (sLe^a) are well established ligands of CD62E, CD62P, and CD62L, also known as E-, P-, and L-selectins, respectively, and are expressed on glycoproteins and glycosphingolipids (for review, see Ref. 1). In human leukocytes and leukemic cells, only sLe^x structures are expressed, and there is no sLe^a expression. sLe^x is expressed on granulocytes, monocytes, and lymphocytes, and importantly its expression on lymphocytes is regulated in a differentiation stage-specific or an activation stage-specific manner (2). The terminal tetrasaccharide structures are synthesized on *N*-acetyllactosamine unit repeats by sequential glycosyltransferase actions (reviewed in Ref. 3). Glycosyltransferases involved in sLe^x structure synthesis are α1→3-fucosyltransferases (α1→3FucT), α2→3-sialyltransferases (α2→3ST), β1→4-galactosyltransferase (β1→4GalT) (4–5) and elongation β1→3-*N*-acetylglucosaminyltransferase (elongation β1→3GnT) (6). Among the five human α1→3FucTs, FucT-VII (7) is expressed in human leukocytes and leukemic cells and has been reported to regulate sLe^x synthesis in human T lymphocytes during T cell activation (8, 9). FucT-IV, termed the "myeloid" α1→3FucT gene is expressed in human granulocytes and myeloid cells and suggested to synthesize Le^x and VIM-2 structures and sLe^x structures (10–11). Four human α2→3STs have been cloned, and among them ST3GalIII and ST3GalIV were reported to synthesize the NeuAcα2→3Galβ1→4GlcNAc structure that is the substrate for α1→3FucTs (12, 13). Attempts to correlate the cell surface expression of sLe^x with the expression of genes encoding α1→3FucTs and α2→3STs and to detect a rate-limiting step for sLe^x structure expression during cell

* This work was supported by Grant-in-Aid for Scientific Research on Priority Areas 05274105 and 09240229 from the Ministry of Education, Science and Culture, Japan, by Grant for General Scientific Research 09670161, and by Research Grant 95KI033 from the Ichiro Kanehara Research Foundation. The costs of publication of this article were defrayed in part by the payment of page charges. This article must therefore be hereby marked "*advertisement*" in accordance with 18 U.S.C. Section 1734 solely to indicate this fact.

§ To whom correspondence should be addressed: Division of Hemopoiesis, Institute of Hematology, Jichi Medical School, Minamikawachi, Tochigi 329-04, Japan. Tel.: 81-285-58-7400; Fax: 81-285-44-7501; E-mail: owlmnaka@jichi.ac.jp.

[1] The abbreviations used are: sLe^x, sialyl-Le^x (sialylated Lewis antigen with Galβ1→4GlcNAc backbone); sLe^a, sialyl-Le^a (sialylated Lewis antigen with Galβ1→3GlcNAc backbone); PA, pyridylamine; PNP, *p*-nitrophenyl; PDMP, D-*threo*-1-phenyl-2-decanoylamino-3-morpholino-1-propanol; BCECF-AM, 2′,7′-bis(carboxyethyl)-5,6-carboxyfluorescein acetomethylester; TPA, 12-*O*-tetradecanoylphorbol-13-acetate; Bz-α-GalNAc, benzyl-α-GalNAc; PAGE, polyacrylamide gel electrophoresis; PBS, phosphate-buffered saline without Ca^{2+}; HPLC, high performance liquid chromatography; PCR, polymerase chain reaction; RT-PCR, reverse transcribed PCR; GAPDH, glutalaldehyde-phosphate dehydrogenase; neo^R, neomycin resistance selection marker; PSGL-1, P-selectin glycoprotein ligand-1; mAb, monoclonal antibody; gp150, 150-kDa glycoprotein; kb, kilobase pair(s); HEPES, 2-[4-(2-hydroxyethyl)-1-piperazinyl]ethanesulfonic acid; MES, 2-(*N*-morpholino)ethanesulfonic acid. Fucosyltransferases and sialyltransferases are designated according to the recommendations of Refs. 45 and 46, respectively. Sugar sequences and glycosphingolipids are designated according to the Nomenclature Committee of the IUPAC (47). Fuc, fucose; Cer, ceramide; C2GnT, UDP-GlcNAc:Galβ1→3GalNAc (GlcNAc to GalNAc) β1→6-*N*-acetylglucosaminyltransferase; C1GalT, UDP-Gal:GalNAc β1→3-galactosyltransferase; C3GnT, UDP-GlcNAc:GalNAc β1→3-*N*-acetylglucosaminyltransferase; C4GnT, UDP-GlcNAc:GlcNAcβ1→3GalNAc (GlcNAc to GalNAc) β1→6-*N*-acetylglucosaminyltransferase; β1→4GalT, UDP-Gal:GlcNAcβ1→3Gal β1→4-galactosyltransferase; α1→3FucT, GDP-Fuc:NeuAcα2→3Galβ1→4GlcNAc α1→3-fucosyltransferase; α2→3ST, CMP-NeuAc:lactoneotetraose α2→3-sialyltransferase; elongation β1→3GnT, UDP-GlcNAc:nLcOse$_4$ β1→3-*N*-acetylglucosaminyltransferase.

differentiation, transformation, and activation have not been definitive (8, 14).

Mechanisms that regulate functional glycosphingolipid expression have been more extensively investigated. For example, we have demonstrated that functional sugar structure synthesis is not regulated through terminal and intermediate glycosyltransferases during differentiation and transformation of human and murine myelogenous leukemia HL-60, K562, and NFS60 cells. Instead, the most upstream glycosyltransferases critically determine terminal carbohydrate structure expression by modulating total flow of glycosphingolipid biosynthesis at upstream branching steps (15–20). In the case of *N*-glycans, branching UDP-GlcNAc:α-D-mannoside β1→6-*N*-acetylglucosaminyltransferase was reported to correlate closely with metastasis (21). In addition, the synthesis of some *O*-glycans is also regulated at a branching step by UDP-GlcNAc:Galβ1→3-GalNAc (GlcNAc to GalNAc) β1→6-*N*-acetylglucosaminyltransferase (core 2 GlcNAc-transferase; C2GnT) in T cell activation and Wiscott-Aldrich syndrome (22, 23). In this context, it would be of great interest to know whether cell surface sLe^x structure expression could be regulated at some branching steps but not at the terminal and elongation steps during cell differentiation.

Human pre-B lymphocytic leukemia cell lines differentiate to a more mature stage upon treatment with 12-*O*-tetradecanoylphorbol-13-acetate (TPA) (24). KM3 is one of these pre-B lymphoid cell lines with such differentiation capability. In the present study, we have investigated down-regulation mechanism of cell surface sLe^x expression using the differentiation system of the KM3 cells. We present here the direct correlation of a branching upstream GlcNAc-transferase, C2GnT, with expression of cell surface sLe^x antigen determinants recognized by KM93 monoclonal antibody (mAb) during differentiation. Furthermore, we report that overexpression of C2GnT cDNA overcomes the effect of phorbolester on the synthesis of sLe^x without changing other phenotypes of the transfected cells.

EXPERIMENTAL PROCEDURES

Chemicals—CMP-[*sialic*-4,5,6,7,8,9-^{14}C]NeuAc (300.9 mCi/mmol), GDP-[*fucose*-U-^{14}C]Fuc (273 mCi/mmol), UDP-[glucosamine-1-^{14}C]GlcNAc (60 mCi/mmol), and UDP-[*galactose*-U-^{14}C]Gal (309.6 mCi/mmol) were obtained from NEN Life Science Products. Unlabeled GDP-fucose (GDP-Fuc) was from Wako Pure Chemicals (Osaka, Japan). Unlabeled CMP-NeuAc, UDP-Gal, and UDP-GlcNAc were from Sigma. Pyridylaminated (PA) oligosaccharides, Galβ1→4GlcNAcβ1→3Galβ1→4-Glc-PA (nLcOse$_4$-PA) and NeuAcα2→3Galβ1→4GlcNAcβ1→3Galβ-1→4Glc-PA (IV^{3}NeuAc-nLcOse$_4$-PA), were prepared as described (25) using nLcOse$_4$ and IV^{3}NeuAc-nLcOse$_4$ that were digested by endoglycoceramidase (Seikagaku, Tokyo, Japan) from nLcOse$_4$Cer and IV^{3}NeuAc-nLcOse$_4$Cer, respectively. nLcOse$_4$Cer and IV^{3}NeuAc-nLcOse$_4$Cer were purified from human erythrocytes. GlcNAcβ1→3-Galβ1→4Glc-PA was prepared from nLcOse$_4$-PA by β-galactosidase digestion. *p*-Nitrophenyl (PNP) oligosaccharides, Galβ1→3GalNAcα1→PNP, Galβ1→3(GlcNAcβ1→6)GalNAcα1→PNP, GalNAcα-1→PNP, and GlcNAcβ1→3GalNAcα1→PNP, were obtained from Toronto Research Chemicals (Toronto, Canada). D-*threo*-1-phenyl-2-decanoylamino-3-morpholino-1-propanol (PDMP) was from Seikagaku (Tokyo, Japan). mAb 8628 against human β1→4GalT protein was prepared as described (26). Guanidinium thiocyanate was purchased from Fluka (Buchs, Switzerland), and CsCl was from Nakarai Tesque (Kyoto, Japan). Fluorescence labeling reagent 2′,7′-bis(carboxyethyl)-5,6-carboxyfluorescein acetomethylester (BCECF-AM) was obtained from Molecular Probes, Inc. (Eugene, OR). All other reagents were of the highest grade commercially available.

Cells and Cell Cultures—Human pre-B leukemia cell line KM3 was kindly supplied by Dr. Jun Minowada (Fujisaki Cell Center, Hayashibara Biochemical Research Institute, Fujisaki, Japan). KM3 cells, the human Burkitt lymphoma cell line Raji, and human myelogenous leukemia HL-60 cells were cultured in RPMI 1640 medium supplemented with 10% fetal calf serum. Differentiation of KM3 cells was carried out by incubating the cells with 8 nM TPA at an initial concentration of 2–5 × 10^5 cells/ml (24). Biosynthesis of glycolipid sugar chains was inhibited by culturing the cells in the presence of 20 μM PDMP for 3 days. For inhibition of *O*-linked sugar chain biosynthesis on glycoprotein, the cells were cultured with 4 mM benzyl-α-GalNAc (Bz-α-GalNAc; Sigma) for 3 days. Inhibition of *N*-linked sugar chain processing was conducted by culturing the cells with 10 μg/ml swainsonine (Genzyme, Cambridge, MA) for 3 days. COS-1 cells were cultured in Dulbecco's modified Eagle's medium supplemented with 10% fetal calf serum.

Flow Cytometry Analysis—Indirect immunofluorescence analyses of cell surface differentiation antigen expression were carried out by FACScan (Becton-Dickinson) as described previously (17). Used monoclonal antibodies were OKBcALLa (CD10; Ortho Diagnostics Systems, Tokyo, Japan), KM93 (CD15s; Seikagaku, Tokyo, Japan), CSLEX-1 (CD15s; ATCC HB8580), 2H5 (CD15s; Pharmingen, San Diego, CA), B9E9 (CD20; Sigma), 4KB128 (CD22; Dako Japan, Kyoto, Japan), SG/73 (VLA-4α; Seikagaku, Tokyo, Japan), B-B15 (LFA1α; T Cell Diagnostics, Cambridge, MA), DF5 (integrin β1; Chemicon International, Temecula, CA), MHL1 (L-selectin; Seikagaku, Tokyo, Japan), and A3D8 (CD44; Sigma). The second antibody was fluorescein isothiocyanate-conjugated goat F(ab′)$_2$ anti-mouse IgG plus IgM (Tago, Inc., Burlingame, CA). Mouse anti-rabbit IgG mAb (IgM) was obtained from Sigma and used as a control first antibody.

Immunoblot Analyses—Immunoblot analyses were performed using anti-sLe^x KM93 mAb or horseradish peroxidase-conjugated anti-human β1→4GalT mAb 8628. Protein was solubilized from cells by a 30-s sonication in 20 mM HEPES buffer (pH 7.2) containing 1% Triton X-100, heated at 100 °C for 5 min in the presence of 2-mercaptoethanol, and subjected to 5% or 10% polyacrylamide gel electrophoresis (PAGE) containing 0.1% SDS. The protein was transferred to Immobilon-P^{SQ} polyvinylidene fluoride membrane (Millipore Corp., Bedford, MA). The antigens were stained and detected by a chemiluminescence reagent kit, Renaissance (DuPont) according to the manufacturer's instructions. As a second antibody, horseradish peroxidase-conjugated goat anti-mouse IgM was used for the detection of KM93-reactive glycoprotein. For calculation of molecular size, prestained and calibrated Kaleidoscope molecular mass standards (Bio-Rad) were used.

Glycosyltransferase Assays—The total membranous fractions were prepared, aliquoted, and stored at −80 °C until use (18). Protein was determined using a Bio-Rad protein assay kit with bovine serum albumin as a standard.

α1→3FucT activities were assayed essentially by the method described for the nLcOse$_4$ β1→3GlcNAc-transferase assay (17) with modification. GDP-[*fucose*-U-^{14}C]Fuc (5.4 μL) was added in a microtube and then dried. In the microtube, 1.68 nmol of cold GDP-Fuc, 20 nmol of NeuAcα2→3Galβ1→4GlcNAcβ1→3Galβ1→4Glc-PA, sodium cacodylate buffer (pH 6.8, 3.75 μmol), $MnCl_2$ (0.63 μmol), Triton CF-54 (75 μg), and the enzyme preparation (100–300 μg of protein) were mixed and incubated at 37 °C for 1–3 h in a total volume of 25 μl. The reaction was stopped by heating at 100 °C for 2 min. The samples were then passed through a 0.22-μm Millipore filter, and an aliquot of each filtrate was applied to a TSK gel ODS-80TM column (4.6 × 150 mm, TOSOH, Tokyo, Japan) and separated by high performance liquid chromatography (HPLC) with a fraction collector. Elution was performed at 50 °C with a 0.1 M acetate buffer (pH 4.0) containing 0.15% *n*-butanol at a flow rate of 1.0 ml/min. Transfer of the radioactive Fuc to the acceptor was determined.

α2→3ST activities were determined as follows. CMP-[*sialic*-4,5,6,7,8,9-^{14}C]NeuAc (2.5 μl) was added in a microtube and then dried. Cold CMP-NeuAc (4.8 nmol), 20 nmol of Galβ1→4GlcNAcβ1→3-Galβ1→4Glc-PA, sodium cacodylate buffer (pH 6.5, 3.75 μmol), Triton CF-54 (75 μg), and the enzyme preparation (100–300 μg of protein) were mixed and incubated at 37 °C for 1–3 h in a total volume of 25 μL. The reaction products were processed and measured as α1→3FucT assays.

β1→4GalT activities were assayed as follows. Cold UDP-Gal (7.5 nmol), 20 nmol of GlcNAc-Galβ1→4Glc-PA, sodium cacodylate buffer (pH 6.8, 3.75 μmol), sodium deoxycholate (2.5 μg), $MnCl_2$ (0.25 μmol), and the enzyme preparation (100–200 μg of protein) were mixed and incubated at 37 °C for 1–3 h in a total volume of 25 μl. The reaction products were processed to HPLC analyses, and the eluates were subjected to quantitation by fluorescence intensity using Gal-PA as a standard.

Elongation β1→3GnT activities were measured as described earlier (17).

C2GnT activities were determined essentially as described (22). Briefly, UDP-[*glucosamine*-1-^{14}C]GlcNAc (0.4 nmol), cold UDP-GlcNAc (24.6 nmol), Galβ1→3GalNAcα1→PNP (25 nmol), and GlcNAc (2.5 μmol) were added in a microtube and then dried. MES buffer (pH 7.0, 3.75 μmol), sodium EDTA (0.25 μmol), Triton X-100 (25 μg), and the

enzyme preparation (100–300 μg) were mixed and incubated in a total volume of 25 μl at 37 °C for 1–3 h. The reaction products were purified by C18 Sep-Pak (Waters, Milford, MA) column chromatography and analyzed by HPLC on a column (0.46 × 25 cm) of PALPACK (type N, TAKARA, Kyoto, Japan). The column was developed isocratically with acetonitrile/water (83:17, v/v). The reaction product was separated and determined as above.

UDP-GlcNAc:GalNAc β1→3-*N*-acetylglucosaminyltransferase (core 3 GnT, C3GnT) and UDP-GlcNAc:GlcNAcβ1→3GalNAc (GlcNAc to GalNAc) β1→6-*N*-acetylglucosaminyltransferase (core 4 GnT, C4GnT) activities were determined as described for C2GnT except for the acceptor substrate using GalNAcα1→PNP and GlcNAcβ1→3GalNAcα1→PNP, respectively. Retention time of GlcNAcβ1→3(GlcNAcβ1→6)-GalNAcα1→PNP was determined as a product of the reaction using porcine colonic mucosal tissue as an enzyme source (27). UDP-Gal: GalNAc β1→3-galactosyltransferase (core 1 GalT, C1GalT) activities were determined as described for C3GnT except for the donor substrate, UDP-[*galactose*-U-^{14}C]Gal and UDP-Gal. The reaction product was analyzed as above.

Semiquantitative Reverse Transcribed PCR Analyses—Total RNA was extracted by the guanidinium CsCl method. Semiquantitative reverse transcribed PCR (RT-PCR) analysis was performed as follows. One μg of RNA was reverse-transcribed by SuperScript II reverse transcriptase (Life Technologies, Inc.) using oligo(dT) primers (Amersham Pharmacia Biotech, Uppsala, Sweden). One-twentieth volume of the reaction mixture was subjected to PCR (total of 50 μl). The reactions were performed using 60 mM Tris-HCl buffer (pH 9.0 for FucT-VII and β1→4GalT, pH 10.0, for ST3GalIII, ST3GalIV, and C2GnT and pH 8.5 for glutalaldehyde-phosphate dehydrogenase (GAPDH)), $MgCl_2$ (1.5 mM for β1→4GalT, ST3GalIII, and GAPDH; 2.0 mM for FucT-VII, ST3GalIV, and C2GnT), 15 mM $(NH_4)_2SO_4$, 250 μM each of dATP, dGTP, and dTTP, and 2 μCi of [α-^{32}P]dCTP in the presence of oligonucleotide primers (10 μM each) specific to the respective cDNAs. The primers used were as follows: FucT-VII (7), 5′-ATG TCT TTG GCC GTG CCA ATG GAC-3′ (forward) and 5′-AGC GGA TCT CAG GCC TGA AAC CAA-3′ (reverse); ST3GalIII (12), 5′-TGA GAC TGA ATT CAG CAC CAG-3′ (forward) and 5′-TCA GAT GCC ACT GCT TAG ATC-3′ (reverse); ST3GalIV (13), 5′-ACA CAC TCC TCG TCC TGG TAG CT-3′ (forward) and 5′-CTA CAG CTC TTG CCC AGG TCA GAA-3′ (reverse); β1→4GalT (5), 5′-CAA GAA GCC TTG AAG GAC TAT G-3′ (forward) and 5′-AAA ACG CTA GCT CGG TGT CCC GAT-3′ (reverse); C2GnT (22), 5′-GCA ATG AGT GCA AAC TGG AAG T-3′ (forward) and 5′-AAT TGC CCG TAA TGG TCA GTG TT-3′ (reverse); and GAPDH (28), 5′-CCA CCC ATG GCA AAT TCC ATG GCA-3′ (forward) and 5′-TCT AGA CGG CAG GTC AGG TCC ACC-3′ (reverse).

5% PAGE was conducted in Tris borate-EDTA buffer at 50 V using one-fifth volume (10 μl) of the PCR reaction mixtures, and the signals were visualized by autoradiography. The results were quantitated with a BAStation Bio-Image Analyzer (Fuji Film, Tokyo, Japan). By extensive control experiments, the PCR cycle numbers were determined for the respective primer pairs so that the amplification efficiency remained constant and the amplified PCR product was directly proportional to the quantity of the used RNA. The selected cycle numbers were 27 for FucT-VII and ST3GalIV, 26 for ST3GalIII and C2GnT, 25 for β1→4GalT, and 20 for GAPDH. The reasons why we took this procedure instead of conventional RNA blot methods or competitive RT-PCR analyses were as follows. (i) The transcript level of glycosyltransferase was very low, and we could hardly observe in detail their changes during TPA treatment by Northern analyses. (ii) It is easy to detect the time-dependent precise changes of the relative amount of each transcript by the semiquantitative RT-PCR method.

Preparation of Full-length C2GnT cDNA and Subcloning to Mammalian Expression Vectors—Full-length human C2GnT cDNA was prepared by PCR cloning. Total RNA from HL-60 cells was reverse-transcribed as above. The cDNA was amplified by 32 cycles of PCR in 60 mM Tris-HCl buffer (pH 8.5), 1.5 mM of $MgCl_2$, 15 mM $(NH_4)_2SO_4$, 250 μM each of dATP, dGTP, dTTP, and dCTP. Primers used were 5′-TTA TTG TTT GAA ATG CTG AGG ACG-3′ (forward) and 5′-TAA TGG TCA GTG TTT TAA TGT CT-3′ (reverse). The amplified C2GnT cDNA was directly subcloned to pCR3 mammalian expression vector and a sense-oriented clone was chosen and designated as pCR3-C2GnT. Sequences of the insert were analyzed by the dideoxy chain termination method (29), and the deduced amino acid sequence was confirmed to be identical to that of human C2GnT (22).

Overexpression of C2GnT cDNA in KM3 Cells—pCR3-C2GnT plasmid was transfected into KM3 cells by electroporation method as described (19). Over 10 monoclonal transfectants were selected and established by G418 resistance and by limiting dilution. Among them, a clone that expressed a maximum level of exogenous C2GnT transcript was chosen and designated as KM3c1e2. The transfected cell line with pCR3 vector alone was also established and designated as KM3m1e3. Expression of exogenous C2GnT was confirmed by PCR analyses using a reverse primer specific to pCR3 vector and a forward primer common to both endogenous and exogenous C2GnT (see Fig. 5*A*; pCR3 vector-specific primer (*V*) and common forward primer (*C*)). Sequences of the common forward primer for C2GnT were the same as that described above. Differential detection of the endogenous C2GnT expression from the exogenous one was conducted by PCR analysis using the common sense primer C and a specific reverse primer for the 3′-untranslated region of C2GnT that were not included by exogenous plasmid sequence (see Fig. 5*A*; reverse primer specific to endogenous transcript (*EN*)). The neomycin resistance selection marker (neo^R) expressed in the transfectants was detected by PCR analyses. Primer sequences were as follows: exogenous C2GnT (pCR3), 5′-GTG ATG GAT ATC TGC AGA ATT C-3′ (reverse); endogenous C2GnT (22), 5′-CTT CTT GTT CAT AAA ATT GCC CG-3′ (reverse); neo^R (30), 5′-TTG TCA CTG AAG CGG GAA GGG A-3′ (forward) and 5′-AAT CGG GAG CGG CGA TAC CGT A-3′ (reverse).

PCR conditions, pH, $MgCl_2$ concentration, and PCR cycle numbers were as follows: pH 8.5, 2.5 mM, 26 cycles for exogenous C2GnT; pH 10.0, 1.5 mM, 27 cycles for endogenous C2GnT; and pH 8.5, 2.0 mM, 22 cycles for neo^R cDNA, respectively.

Preparation of E-selectin-transfected COS-1 Cells—Total RNA was extracted from human umbilical vein endothelial cells treated with recombinant IL-1β at 10 units/ml concentration for 4 h, and 1 μg of RNA was reverse-transcribed as described above. The full-length human E-selectin cDNA was prepared by 32 cycles of PCR amplification in 60 mM Tris-HCl buffer (pH 9.0), 1.5 mM of $MgCl_2$, 15 mM $(NH_4)_2SO_4$, 250 μM each of dATP, dGTP, dTTP, and dCTP. Used primers were 5′-AAG TCA TGA TTG CTT CAC AGT TT-3′ (forward) and 5′-AAC TTA AAG GAT GTA AGA AGG C-3′ (reverse) (31). The amplified cDNA was directly subcloned to pCR3 expression vector, and a sense-oriented clone was chosen and designated as pCR3-E-selectin. The plasmid was transfected into COS-1 cells by the electroporation method as described (19), and the monoclonal transfectant was selected as above and designated as COS1E5 cells. E-selectin expression was confirmed by flow cytometry analysis and RNA blot methods (data not shown). The COS1 derivative cell line transfected with the vector alone, pCR3, was also prepared and designated as COS1m cells.

Low Shear Force COS Cell Adhesion Assay—After treatment with 4 mM Bz-α-GalNAc for 3 days or 8 nM TPA for 4 days, KM3 cells were harvested, washed with PBS three times, labeled with BCECF-AM at 37 °C for 15 min (32), washed with PBS twice, pretreated with or without anti-sLe^x mAb (KM93) or the control mAb (mouse anti-IgG; Sigma), washed with PBS twice, and then resuspended in unsupplemented RPMI 1640 medium. Separately, 2.2 × 10^6 COS1E5 cells were seeded and cultured on a cover glass in 35-mm dishes (assay plate) for overnight. After washing the COS1E5 cells twice with unsupplemented RPMI 1640 and pretreating the cells with or without anti-E-selectin mAb (1.2B6; T Cell Diagnostics, Cambridge, MA) or the control mAb (mouse anti-IgG; Sigma), a low shear force COS cell adhesion assay was performed as reported (33) with sight modification. On the layer of COS1E5 cells, 1 × 10^6 of the above labeled KM3 cells (in 0.6 ml of medium) were placed. The cells were incubated on a constantly rocking platform for 15 min at 4 °C, and the plates were washed five times with unsupplemented RPMI 1640 followed by fixation with cold 0.4% formaldehyde/RPMI 1640. The cover glass was removed from the assay plate bottom and placed on the slide glass. The fluorescence-labeled cells were counted on a fluorescence microscope system (BX-60/BX-FLA; Olympus, Tokyo, Japan), and the mean number of cells bound to COS1E5 cells/cm^2 was determined.

RESULTS

sLe^x Antigen Expression in KM3 Cells before and after TPA Treatment—Upon treatment of KM3 cells with 8 nM TPA, cell growth was significantly suppressed within a day (24). Expression of CD10, CD22, and CD20 was characterized before and after treatment (Fig. 1*A*, *left*). All three antigens are used as pre-B cell markers. However, CD22 and CD20 are known as more mature markers than CD10. While CD10 expression was very high in KM3 cells before treatment, the expression significantly decreased after treatment for 3 days. On the other hand, CD22 was obviously up-regulated after treatment. In addition, while CD20 was negative in KM3 cells before treat-

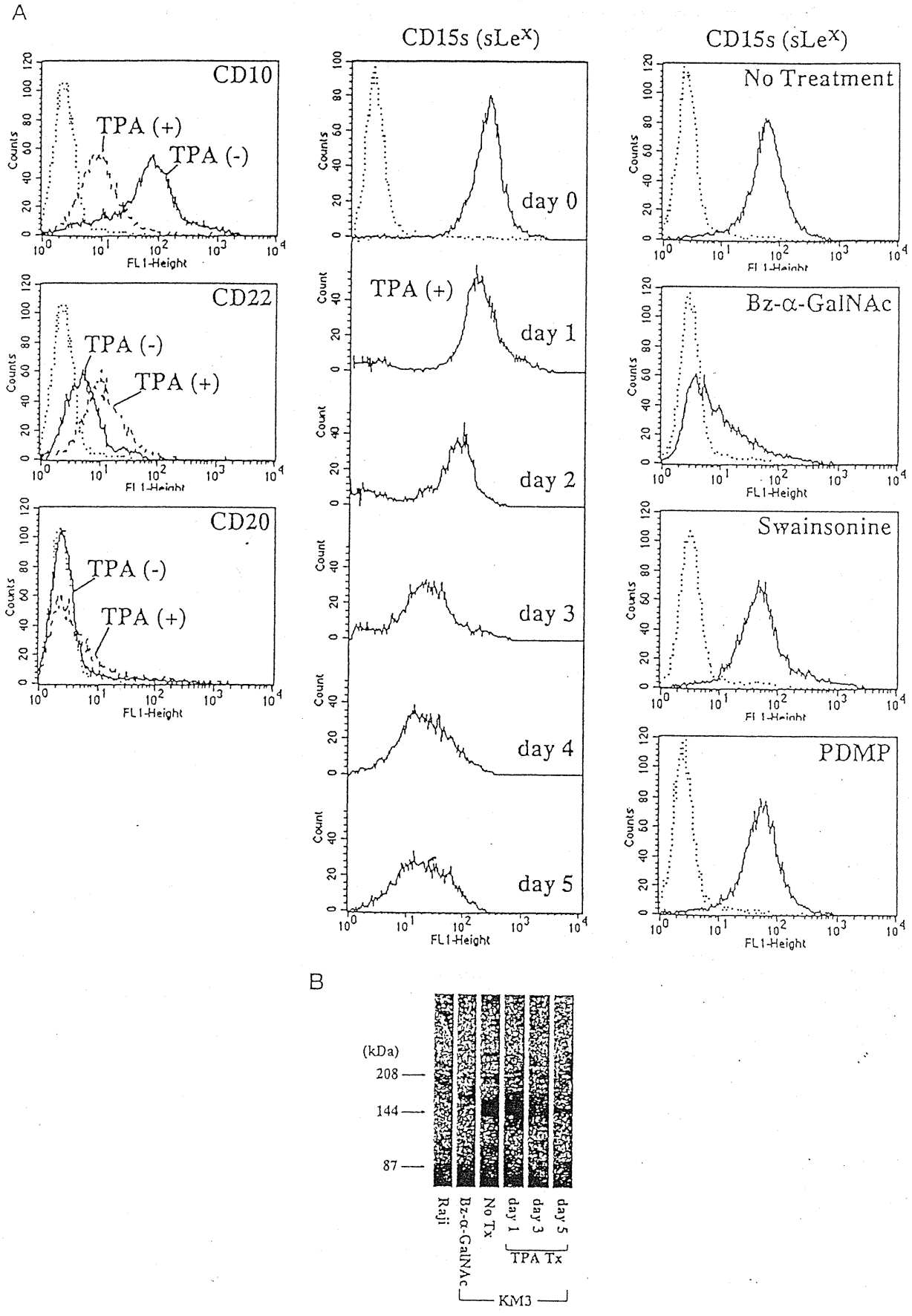

FIG. 1. *A*, expression analyses of CD10, CD22, CD20, and CD15s in KM3 cells by FACScan. *Left column* (from *top* to *bottom*), CD10, CD22, and CD20 reactive cells, respectively. *Solid*, *broken*, and *dotted lines* in the *left column* represent the histograms of positive cells without TPA

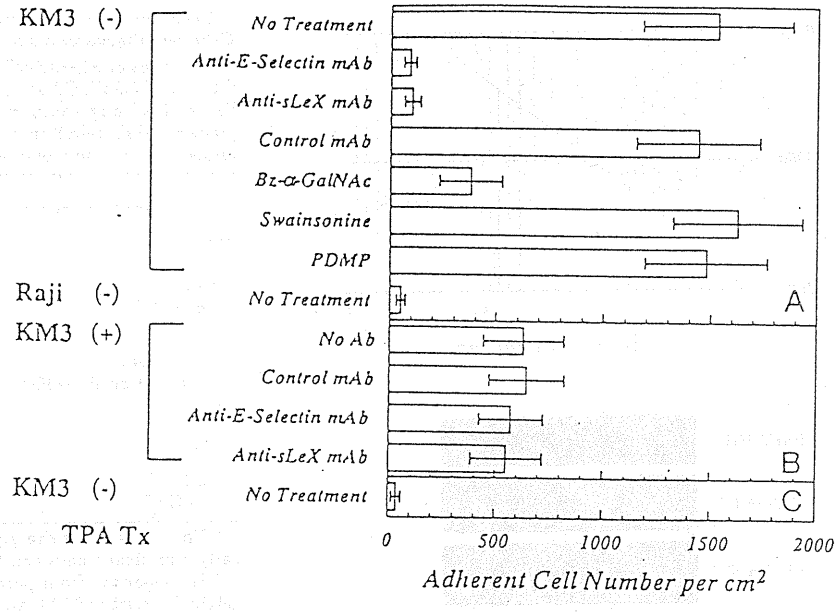

FIG. 2. Low shear force COS cell adhesion analyses of KM3 cells. Cells were treated with TPA or inhibitors, labeled with BCECF-AM (32), pretreated with or without anti-sLe^x mAb (KM93) or control mAb (mouse anti-IgG; Sigma), and resuspended in unsupplemented RPMI 1640. Separately, COS1E5 cells were pretreated with or without anti-E-selectin mAb or the control mAb. Then low shear force COS cell adhesion assay was performed (33) as described under "Experimental Procedures." *A* and *B*, analyses using the COS1E5 cells; *C*, analysis using the mock-transfected COS1m cells. The values are expressed as an average ± S.E. of three experiments.

ment, the expression slightly increased after treatment. Consequently, it was thought that KM3 cells were differentiated into a more mature stage by TPA treatment as described (24). Subsequently, sLe^x expression was investigated in the cells. As shown in Fig. 1*A* (*middle*), the cells were highly reactive with KM93 mAb before treatment. However, the reactivity significantly decreased in a time-dependent manner: no significant change at day 1, slightly decreased at day 2, and markedly down-regulated at day 3. After that, however, no further decrease was observed at days 4 and 5. The extent of the decreased KM93 reactivity at days 3–5 was about ⅛ to 1/12 of the control (calculated by the mean fluorescence intensity), although the results fluctuated from experiment to experiment. By contrast to the mAb KM93, KM3 cells were not stained at all by other mAbs against sLe^x structures, CSLEX-1, and 2H5.

Expression of sLe^x Structures on O-Glycosylated Protein—The highly expressed sLe^x antigen significantly decreased by Bz-α-GalNAc treatment for 3 days as well, while 3 days' treatment of the cells by swainsonine or PDMP did not show any change in KM93 reactivity at all (Fig. 1*A*, *right*). This clearly indicates that sLe^x structures on KM3 cells are exclusively located on the *O*-linked oligosaccharide chains. Subsequently, we tried to detect glycoproteins expressing sLe^x antigen determinant by immunoblot analyses (Fig. 1*B*). While no signal was observed in sLe^x-negative Raji cells, a glycoprotein with an apparent molecular size of ~150 kDa (designated as gp150) was clearly detected in the positive KM3 cells. Although two minor proteins with molecular sizes of ~250 and ~200 kDa were also visualized, no other band was noticed on the 5% gel (*third lane*; *No Tx*) and even on the 10% gel (data not shown). Upon treatment with Bz-α-GalNAc, the major and minor glycoproteins almost completely disappeared as shown in the *second lane*. This also indicates that sLe^x structures are located on *O*-linked oligosaccharide chains of glycoproteins and correlates with the results presented by flow cytometry analyses (Fig. 1*A*, *right*). In addition, we also analyzed the effects of TPA treatment for 1, 3, and 5 days (Fig. 1*B*, *right three lanes*). The intensity of gp150 and the other minor proteins significantly reduced in a time-dependent manner and completely disappeared at day 5. These results also correlated with the flow cytometry results (Fig. 1*A*, *middle*).

TABLE I
Flow cytometry analyses of cell adhesion molecule expression
Cell surface expression of VLA4, LFA1α, integrin β1, L-selectin, and CD44 on KM3 cells treated with or without TPA for 4 days was analyzed using specific mAbs. The expression was shown in a semiquantitative manner: ++++, positive cells were more than 80%; +++, 40–80% positive; ++, 20–40% positive; +, 5–20% positive; ±, 1–5% positive; −, positive cells were less than 1%.

	KM3 without TPA	KM3 with TPA
VLA4	++++	++++
LFA1α	−	±
Integrin β1	+	+
L-selectin	++	++
CD44	−	±

Low Shear Force COS Cell Adhesion Analyses of KM3 Cells—Roles of cell surface sLe^x on KM3 cells were investigated as summarized in Fig. 2 using COS1E5 cells that permanently expressed E-selectin. KM3 cells adhered to COS1E5 cells (Fig. 2*A*, *uppermost bar*), while sLe^x-negative Raji cells did not exhibit cell adhesion (*bottom bar*). For another control, sLe^x-positive KM3 cells did not adhere to COS1m cells transfected with the vector pCR3 alone (Fig. 2*C*). As shown in Fig. 2*A*, this adhesion was blocked by anti-E-selectin mAb or by anti-sLe^x mAb KM93. In addition, Bz-α-GalNAc treatment significantly abolished KM3 cell adhesion to COS1E5 cells, while swainsonine and PDMP had no effect on the adhesion. The number of adherent KM3 cells decreased with TPA treatment (Fig. 2*B*, *uppermost bar*). Although the percentage of adherent KM3 cells treated with TPA was about 40% and higher than those of Bz-α-GalNAc-treated cells (25%), the decrease in the adherent

treatment, positive cells with TPA treatment for 3 days, and control cells, respectively. *Middle column*, time-dependent decrease (from day 0 to day 5) in CD15s positivity of KM3 cells treated with TPA. *Right column* (from *top* to *bottom*), CD15s positive cells grown without any treatment, with treatment of 4 mM Bz-α-GalNAc, 10 μg/ml swainsonine, and 20 μM PDMP for 3 days, respectively. *Solid* and *dotted lines* in the *right column* represent the histograms of positive cells and control cells, respectively. The *ordinate* and *abscissa* represent cell numbers and relative fluorescence intensity, respectively. *B*, immunoblot analyses of KM93-reactive glycoprotein in KM3 cells. Forty μg of protein was prepared and subjected to 5% PAGE followed by transfer to Immobilon P^{SQ} membrane and by staining with KM93 mAb. The signal was detected by the chemiluminescence method. The *arrows* indicate the positions of molecular mass standards.

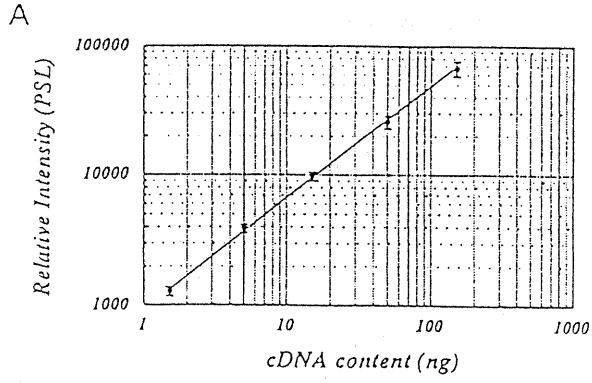

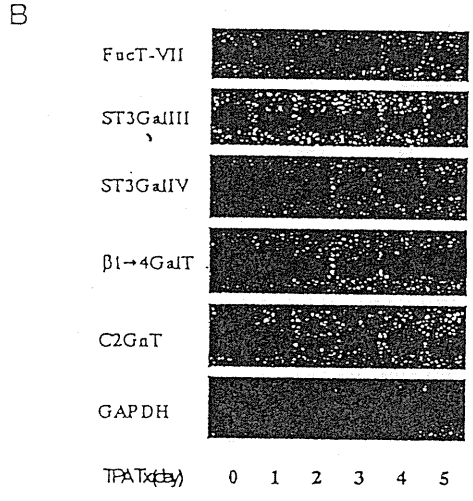

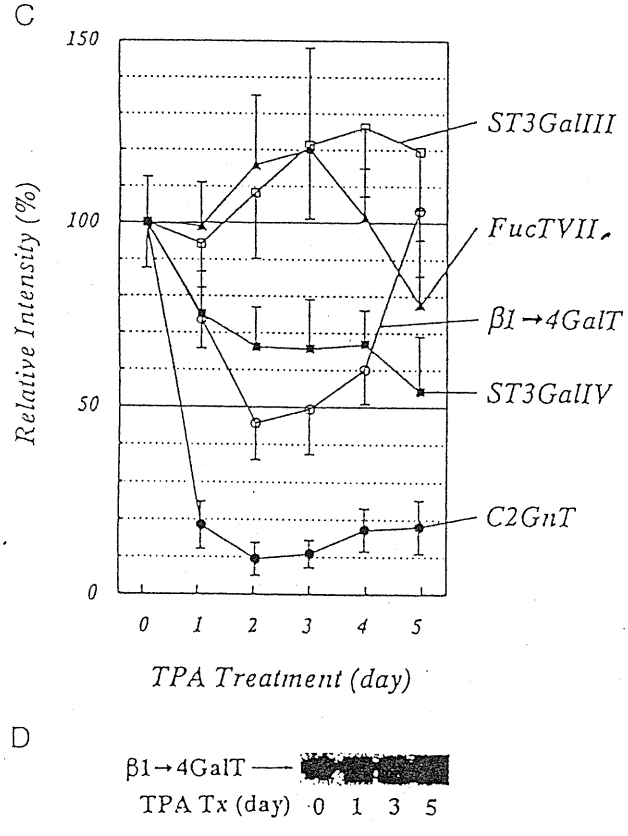

FIG. 3. *A*, a control experiment showing the linearity of RT-PCR analysis. After fixing the PCR conditions including the cycle numbers, RT-PCR experiments were conducted using primer pairs for C2GnT and cDNA corresponding to 1.5–150 ng of RNA. The products were quantitated by BAStation. Values are means ± S.D. of the results of three separate experiments and are presented as relative intensity (photostimulated luminescence units; *PSL*). *B* and *C*, semiquantitative RT-PCR analyses of glycosyltransferases involved in sLe^x structure synthesis during TPA-induced differentiation of KM3 cells. RNA from TPA-treated KM3 cells was reverse-transcribed, and cDNA was subjected to PCR. PAGE was conducted, and the products were quantitated by BAStation and visualized by autoradiography (FucT-VII, 0.44 kb; ST3GalIII, 0.5 kb; ST3GalIV, 0.47 kb; β1→4GalT, 0.5 kb; C2GnT, 0.6 kb; GAPDH, 0.6 kb). Value of each PCR product was normalized by GAPDH and is expressed as mean ± S.D. of three separate experiments and as relative intensity (%) compared with the data at day 0. *D*, immunoblot analyses of β1→4GalT enzyme protein. Forty μg of protein from TPA-treated KM3 cells was prepared and subjected to 10% PAGE followed by transfer to Immobilon P^{SQ} membrane and by staining with horseradish peroxidase-conjugated 8628 mAb. The *arrow* indicates the position of the β1→4GalT protein.

TABLE II

Glycosyltransferase activities involved in the synthesis of sLe^x and O-linked oligosaccharide core structure in KM3 cells treated with TPA

Activities of α1→3FucT, α2→3ST, β1→4GalT, elongation β1→3GnT, C1GalT, C2GnT, C3GnT, and C4GnT were determined using respective PA- or PNP-oligosaccharides as acceptors. The values are expressed as pmol/mg of protein/h and as means of triplicate assays ± S.D. Statistical analyses were conducted with Student's *t* test; *, $p < 0.01$.

Glycosyltransferase	KM3	
	No treatment	TPA treatment
	pmol/mg protein/h	
α1→3FucT[a]	6.8 ± 0.8	7.5 ± 1.0
α2→3ST[a]	10.8 ± 1.8	8.3 ± 1.2
β1→4GalT	207.0 ± 32.1	325.7 ± 7.8 *
Elongation β1→3GnT[a]	42.7 ± 9.2	29.5 ± 5.9
C1GalT[a]	2285 ± 541	1880 ± 307
C2GnT	338 ± 28	36.2 ± 3.2 *
C3GnT[b]	ND[c]	ND
C4GnT[b]	ND	ND

[a] The values of these glycosyltransferase activities were not statistically significant between the control and TPA treatment.

[b] Homogenate from porcine colon mucosa had very high C3GnT and C4GnT activity of 12.0 and 10.3 nmole/mg protein/hr, respectively (27).

[c] ND, not detected.

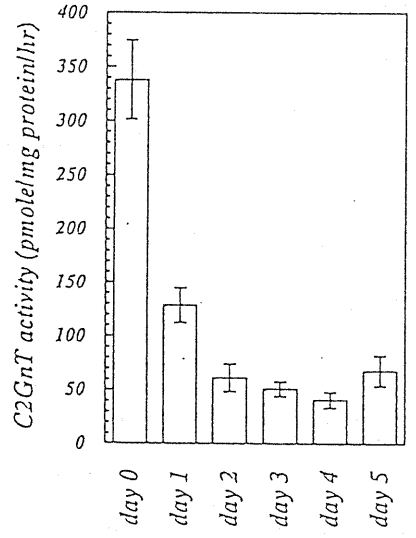

FIG. 4. C2GnT enzyme activities during TPA-induced differentiation of KM3 cells. Cells were treated by 8 nM TPA for the time indicated. Activities of C2GnT were measured using PNP-oligosaccharide as an acceptor (22). C2GnT enzyme activity is expressed as mean ± S.D. of three separate experiments.

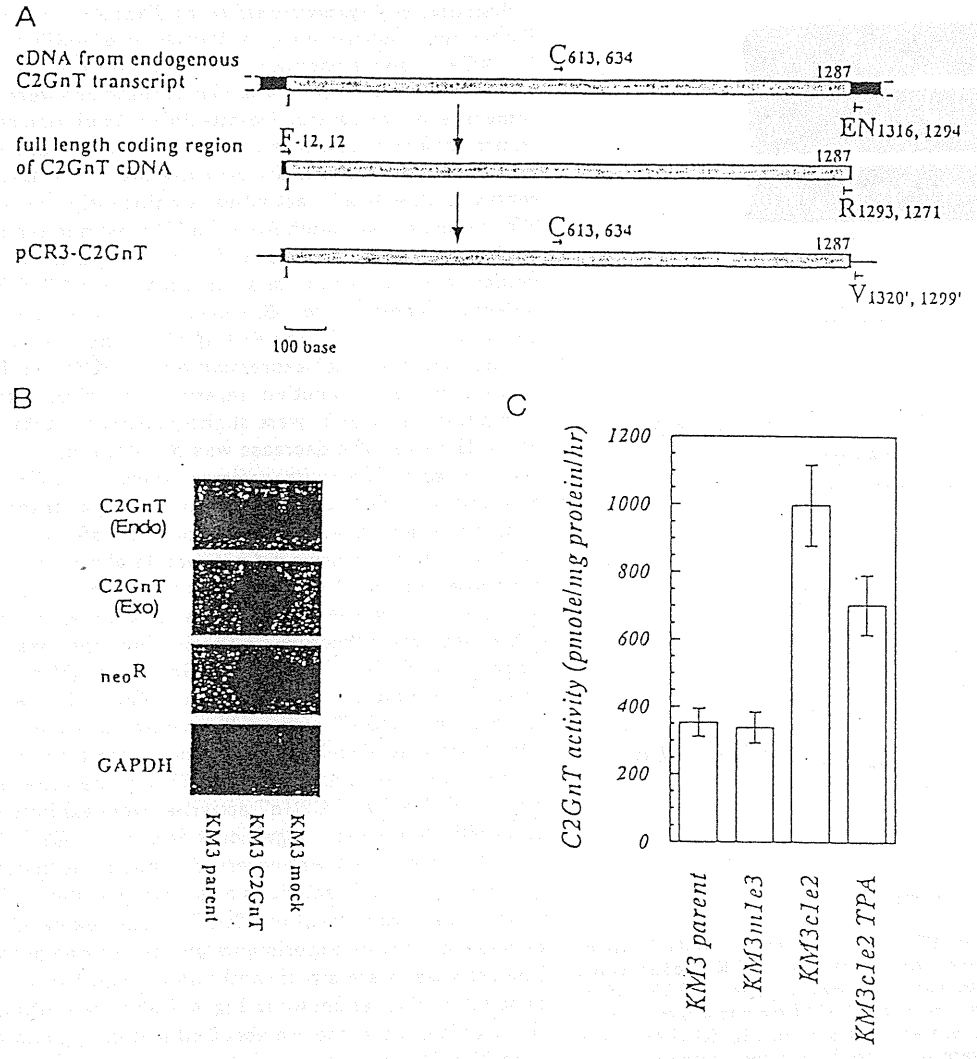

FIG. 5. Overexpression of C2GnT cDNA in KM3 cells. *A*, scheme of differential detection of exogenous C2GnT transcript from endogenous one. *Upper bar*, C2GnT cDNA from endogenous transcript; *middle*, full-length coding region of the cDNA; *lower*, pCR3-C2GnT plasmid. *Hatched boxes*, 1287-base-long coding region with nucleotide number counting from the starting point of the region; *closed bars*, 5′- (*left*) and 3′- (*right*) untranslated regions of C2GnT cDNA; *lines* in the *lower part*, pCR3 vector portion. The *horizontal arrows* with *characters* represent the positions and directions of primers used in this work. *F* and *R*, forward and reverse primers for full-length cDNA, respectively. *C*, common forward primer for endogenous and exogenous transcript detection; *EN*, reverse primer specific to the endogenous transcript; *V*, reverse primer specific to the vector. The *numbers* after each character represent the start and end nucleotide positions of the primer, respectively. The position of the 5′-untranslated side is expressed as a negative number, and positions of the 3′-untranslated side in the vector sequence are expressed as primed numbers. The full-length coding region was prepared from cDNA from the endogenous transcript using the primers F and R and subcloned to pCR3 vector (indicated by the *vertical arrows* from the *upper* to *lower illustrations*). *B*, RT-PCR analyses of overexpressed C2GnT in the transfected cells. RNA was reverse-transcribed, and cDNA was subjected to PCR reaction. PAGE was conducted, and the bands were visualized by autoradiography. *C2GnT (Endo)* and *C2GnT (Exo)*, endogenous (0.7 kb) and exogenous C2GnT (0.7 kb), respectively. neo^R was 0.5 kb, and GAPDH wsa 0.6 kb. *C*, C2GnT activities in the transfected KM3 cells. The transfected cells were treated with or without 8 nM TPA for 4 days. Activities of C2GnT were measured using PNP-oligosaccharide as an acceptor (22). C2GnT enzyme activity is expressed as mean ± S.D. of three separate experiments.

cell numbers was significant compared with those of no treatment control. To investigate why 40% binding remains after TPA treatment despite the dramatic down-regulation of sLe^x expression (Fig. 1, *A* and *B*), we conducted another cell adhesion blocking experiment. Neither anti-E-selectin nor anti-sLe^x mAb further blocks the binding of TPA-treated KM3 cells (Fig. 2*B*). Since this suggested that the remaining 40% binding is due to other factor(s) than E-selectin, we examined possible cell adhesion molecule expression in TPA-treated KM3 cells using FACScan. As summarized in Table I, we found no significant up-regulation of VLA4, LFA1α, integrin β1, L-selectin, and CD44 by TPA treatment. Therefore, in addition to E-selectin, we think that alternative adhesion molecule(s) may mediate binding in our COS cell assay after TPA treatment.

Semiquantitative RT-PCR Analyses of Glycosyltransferase Expression—The above results suggested that sLe^x determinants are mainly located on *O*-glycosylated gp150 and that the sLe^x structures on the protein play an important role in E-selectin-mediated cell adhesion. Therefore, expression of glycosyltransferase gene transcripts involved in the biosynthesis of sLe^x was analyzed by semiquantitative RT-PCR analyses. Fig. 3*A* is a typical example of a control experiment demonstrating that the amplified PCR product (C2GnT) was directly proportional to the quantity of used cDNA content. For other PCR products, we have conducted similar experiments and determined that the products were proportional to cDNA amounts (data not shown). Subsequently, expression of FucT-VII, ST3GalIII, ST3GalIV, β1→4GalT, and C2GnT was examined using total RNA of TPA-treated KM3 cells, as shown in Fig. 3, *B* and *C*. Standard GAPDH was constitutively amplified, and

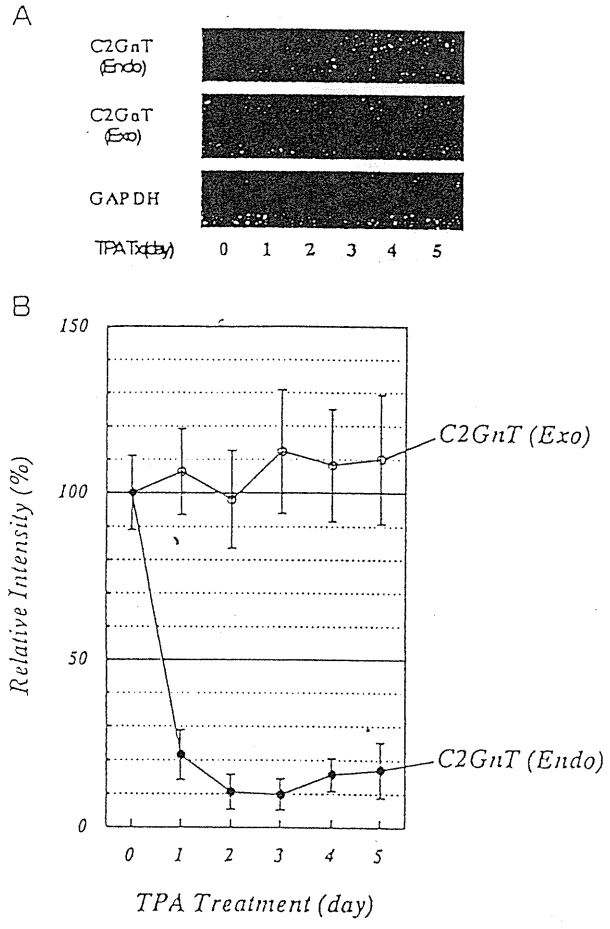

FIG. 6. Semiquantitative RT-PCR analyses of C2GnT transcripts during TPA-induced differentiation of KM3c1e2 cells. RNA was reverse-transcribed, and cDNA was subjected to PCR. Differential detection of the exogenous (*Exo*; 0.7 kb) from endogenous (*Endo*; 0.7 kb) C2GnT was carried out as illustrated in Fig. 5*A*. PAGE was conducted, and the bands were visualized by autoradiography (*A*). The quantitated value of each PCR product was normalized by GAPDH and is expressed as mean ± S.D. of three separate experiments and as relative intensity (percentage) compared with the data at day 0 (*B*).

its radioactivity levels were used for normalization of glycosyltransferase expression. FucT-VII PCR product was clearly observed at day 0, and the expression did not show significant change during differentiation, although its level was slightly enhanced at days 2 and 3. PCR product of ST3GalIII was also observed and constitutively expressed during differentiation by TPA. On the other hand, the expression of ST3GalIV and β1→4GalT transcripts was down-regulated to ⅔ and ½ levels during differentiation, respectively, especially at days 2 and 3. At day 5, however, expression of β1→4GalT recovered to its original level. Surprisingly, C2GnT expression showed more drastic change than ST3GalIV and β1→4GalT. Expression level of C2GnT transcript was down-regulated in a time-dependent manner to ⅕ at day 1 and to 1/10 at days 2 and 3, although the level recovered slightly at days 4 and 5.

Immunoblot Analyses of β1→4GalT Protein—To examine expression of β1→4GalT in protein level during TPA treatment, immunoblot analyses were performed using anti-human 8628 mAb (Fig. 3*D*). A substantial amount of β1→4GalT protein was exhibited before TPA treatment. While expression of the transcript was down-regulated to ½ the level of the control, β1→4GalT enzyme protein level did not show any decrease during differentiation. Instead, time-dependent increase was observed during TPA treatment.

Activities of Glycosyltransferases That Are Involved in sLe^x Expression—Subsequently, activities of α1→3FucT, α2→3ST, β1→4GalT, and elongation β1→3GnT were examined (Table II). α1→3FucT activities after TPA treatment were almost the same level as the control. Despite down-regulation of ST3GalIV transcript and cell surface sLe^x levels at days 3 and 4, α2→3ST activities did not markedly decrease after TPA treatment. By contrast, β1→4GalT activities significantly increased after TPA induction, although β1→4GalT transcript and cell surface sLe^x levels were down-regulated after treatment. Taken together with the results of semiquantitative RT-PCR and immunoblot analyses for β1→4GalT, it was suggested that α1→3FucT, α2→3ST, and β1→4GalT do not hold any key role on the control of sLe^x expression during KM3 cell differentiation. Activities of another intermediate glycosyltransferase, elongation β1→3GnT, were slightly decreased after differentiation. However, the decrease was not significant.

Activities of Glycosyltransferases Involved in Core Structure Synthesis of O-Glycans—Since activity and/or transcript levels of terminal and intermediate glycosyltransferases involved in sLe^x structure synthesis did not completely correlate with sLe^x expression and sLe^x determinants were mainly on *O*-glycosylated gp150, it was of great interest to analyze the mechanism of *O*-glycan core structure synthesis. Therefore, we determined activities of C1GalT, C2GnT, C3GnT, and C4GnT before and after TPA-induced differentiation (Table II). Activities of C3GnT and C4GnT were not detected at all in control and TPA-treated KM3 cells, while homogenate from porcine colon mucosa had very high activity (27). On the other hand, substantial C1GalT and C2GnT activities were exhibited in control KM3 cells. Moreover, a significant decrease in C2GnT activities after TPA treatment was observed, while no such decrease was detected in C1GalT activities as shown in Table II. To confirm further the involvement of C2GnT in sLe^x expression, we conducted time course experiments on the enzyme activity levels. The activities were significantly down-regulated in a time-dependent manner as shown in Fig. 4. Compared with the control, the activities decreased to about 40% at day 1, and 10–18% at days 2–4. However, the activities at day 5 were slightly recovered from that at day 4. These results strongly suggest a direct correlation of C2GnT with sLe^x expression, taken together with the results of flow cytometry, immunoblot (see Fig. 1), and RT-PCR analyses (see Fig. 3).

Overexpression of C2GnT in KM3 Cells—Since the suggested direct correlation of C2GnT with expression of sLe^x-bearing *O*-glycan on gp150 seemed to be the most critical, we conducted overexpression experiments of C2GnT cDNA in KM3 cells. C2GnT- and mock-transfected KM3c1e2 and KM3m1e3 cells were established, respectively. First, we tried to perform differential detection of endogenous and exogenous C2GnT transcripts using RNA blot analyses. However, there were two endogenous transcripts in KM3 cells (4.8 and 2.1 kb); the overexpressed exogenous transcript was almost the same size as the smaller endogenous one, and we could not exactly differentiate the exogenous transcript from the endogenous one. Therefore, differential detection was conducted by RT-PCR analyses as illustrated in Fig. 5*A* (see the figure legend and "Experimental Procedures"). As summarized in Fig. 5*B*, the exogenous C2GnT expression was not confirmed in the parental KM3 and mock-transfected KM3m1e3 cells but in the KM3c1e2 cells, while the endogenous C2GnT transcript was detected in all three cell lines. On the other hand, the neo^R gene transcript was detected in KM3c1e2 and KM3m1e3 cells, while the transcript was not exhibited in the parental KM3 cells. In addition, about 3-fold higher C2GnT activities were detected in the transfected KM3c1e2 cells than in the parental KM3 cells, as

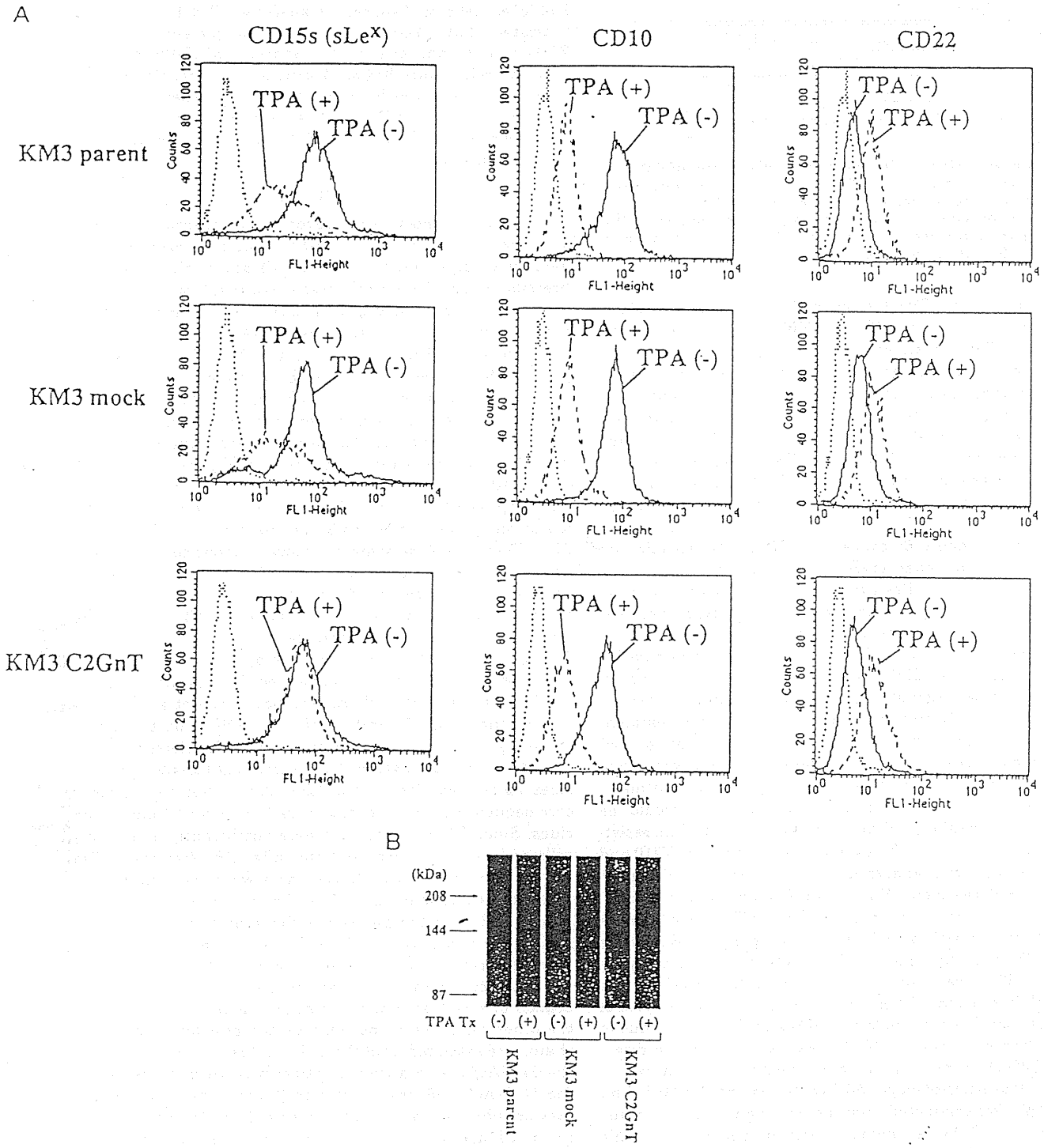

FIG. 7. *A*, FACScan analyses of CD15s (*left column*), CD10 (*middle column*), and CD22 (*right column*) on C2GnT-transfected cells during TPA treatment. *Top row*, parental KM3; *middle row*, mock-transfected KM3m1e3 cells; *bottom row*, C2GnT-transfected KM3c1e2 cells. *Solid*, *broken*, and *dotted lines* represent histograms of positive cells without treatment, positive cells with TPA treatment, and control cells, respectively. The *ordinate* and *abscissa* represent cell numbers and relative fluorescence intensity, respectively. *B*, immunoblot analyses of KM93-reactive glycoprotein in the transfected KM3c1e2 cells treated with TPA. Forty μg of protein was prepared and subjected to 5% PAGE followed by transfer to Immobilon-P^{SQ} membrane and by staining with KM93 mAb. The signal was detected by chemiluminescence method. The *arrows* indicate the positions of molecular mass standards.

shown in Fig. 5*C*. On the other hand, the mock-transfected KM3m1e3 cells expressed the same amount of activities as the parental cells. These results indicate that the exogenous C2GnT is expressed not only in the transcript form but also enzymatically or functionally in the transfected KM3c1e2 cells.

Effect of Phorbolester on Glycosyltransferase and sLe^x Expression in KM3c1e2—Using KM3c1e2 cells, expression of glycosyltransferase transcripts involved in sLe^x structure synthesis were characterized during differentiation. Upon TPA treatment, the endogenous C2GnT transcript level was down-regulated in the transfectant, KM3c1e2 cells, in a time-dependent manner just as in the parental KM3 cells (Fig. 6, *A* and *B*; compare Fig. 3, *B* and *C*). However, exogenous C2GnT was expressed constitutively, and the expression level did not

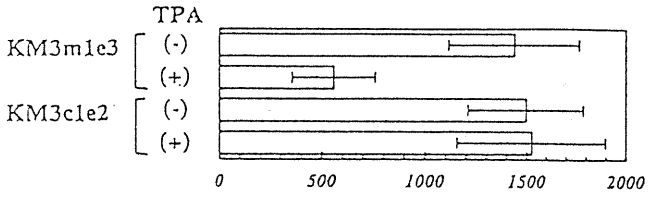

FIG. 8. Low shear force COS cell adhesion analyses of KM3c1e2 cells. Cells treated with 8 nM TPA for 4 days were labeled with BCECF-AM and resuspended in unsupplemented RPMI 1640. Then a COS cell adhesion assay under low shear stress was conducted (33) as described under "Experimental Procedures." The value is expressed as an average ± S.E. of the means of three experiments.

change at all during TPA treatment (Fig. 6, *A* and *B*). Moreover, enzyme activities of C2GnT in KM3c1e2 cells were down-regulated by TPA treatment, but the activity levels in the TPA-treated or -nontreated KM3c1e2 cells were significantly higher than those in the nontreated parental KM3 and mock-transfected KM3m1e3 cells (Fig. 5*C*). On the other hand, expression patterns of α1→3FucT, ST3GalIII, ST3GalIV, and β1→4GalT transcripts in TPA-treated KM3c1e2 cells were almost the same as those in the parental KM3 cells, especially in that the levels were not augmented at days 2–4 (data not shown).

Subsequently, effect of exogenous C2GnT transfection on sLe^x expression was characterized using the transfected cell liens treated with TPA. Results of the flow cytometry analyses are summarized in Fig. 7*A*, *left column*. sLe^x expression was down-regulated in the mock-transfected KM3m1e3 cells as in the parental KM3 cells upon TPA treatment (*top* and *middle*). In C2GnT-transfected KM3c1e2 cells, however, sLe^x expression was not down-regulated by TPA treatment, and the expression level was almost the same as that of no-treatment control (*bottom*). There was a possibility that this block of sLe^x expression down-regulation in the transfected cells was due to the cell surface phenotypic change before the TPA treatment; *i.e.* according to the transfection, KM3c1e2 cells could be thought to lose capability of differentiation and become resistant to the TPA treatment. To exclude the possibility, CD10 and CD22 expression was analyzed in the transfected KM3c1e2 cells after TPA treatment (Fig. 7*A*, *middle* and *right columns*). CD10 expression was down-regulated after TPA treatment in KM3c1e2 cells as well as KM3m1e3 and parental KM3 cells (*middle*). On the other hand, CD22 expression was up-regulated after TPA treatment in KM3c1e2 cells as well as the control cell lines (*right*). These results suggest that the block of sLe^x expression down-regulation in KM3c1e2 cells is not due to acquiring the resistancy to TPA treatment but to the direct effect of C2GnT transfection on sLe^x synthetic machinery.

Effect of Phorbolester on gp150 Expression and Cell Adhesion of KM3c1e2—We conducted immunoblot analyses in the transfected cells after TPA treatment, as presented in Fig. 7*B*. While gp150 was significantly decreased in its intensity after TPA treatment in the parental KM3 and mock-transfected KM3m1e3 cells, the protein of the C2GnT-transfected KM3c1e2 cells did not disappear. Instead, the intensity of gp150 in TPA-treated KM3c1e2 cells was as strong as that of the no-treatment control. This was also in a good agreement with the flow cytometry data (Fig. 7*A*, *left column*) and indicates that C2GnT transfection results in remodeling of the sLe^x synthetic machinery in KM3c1e2 cells.

Finally, we tested the possible effect of C2GnT transfection on cell adhesion capability using low shear force COS cell adhesion assay (Fig. 8). Like KM3 parent cells, adhesion of KM3m1e3 cells was significantly inhibited by TPA treatment. By contrast, TPA treatment had no effect on cell adhesion of KM3c1e2 cells to E-selectin-transfected COS1E5 cells. This indicated that C2GnT transfection completely blocked the TPA-induced inhibition on cell adhesion of KM3c1e2 cells to COS1E5 cells. Since KM3c1e2 cells had no phenotypic change from the parental cells except for sLe^x synthetic machinery (Fig. 7), the block of TPA-induced inhibition on cell adhesion must be due to a direct effect of C2GnT transfection on the sLe^x synthetic machinery.

DISCUSSION

T and B lymphocytes are reported to undergo an antigenic shift from immature sLe^x positive status to negative status along with differentiation (2). In this study, sLe^x antigen expression on pre-B KM3 cells was down-regulated during B cell maturation with TPA (Fig. 1). This was in good agreement with previous results. There are several mAbs against sLe^x structures including FH-6, CSLEX-1, and 2H5 (2). Among them, mAb KM93 has been introduced by Hanai *et al.* (34) and used for the expression cloning of FucT-VII (7). Although sLe^x is highly expressed and easily detected by the different antibodies in human granulocytes, monocytes, and myelogenous and monocytic leukemia cells, expression of CD15s recognized by each mAb is somewhat different from each other in human lymphocytes (2). According to the present results, KM3 cells are strongly positive for KM93 but negative for CSLEX-1 and 2H5. There must be some structural differences between the epitopes recognized by KM93 and by CSLEX-1 or 2H5. As far as relationship between KM93-reactive sLe^x and glycosyltransferase expression is concerned, however, C2GnT is surely thought as a "key" glycosyltransferase.

O-Glycans have been reported to play important roles on cell adhesion, and multivalency presented by *O*-glycans is thought as one of the essential characteristics to potentiate cell adhesion strength (35). Therefore, sLe^x structures on the *O*-glycosylated gp150 may play a central role for E-selectin-mediated cell adhesion in our system. Structures of *O*-linked oligosaccharides have been classified on the basis of their fundamental core sequences; core 1, core 2, core 3, and core 4 oligosaccharides. Since C1GalT activities were significantly high in KM3 cells and were not down-regulated after TPA treatment (Table II), the synthesis of core 2 sequences would take place in the presence of abundant C2GnT activities and its acceptor substrate, and it would determine the synthetic velocity of the remaining structures in the downstream biosynthetic pathways. Therefore, sLe^x may be created on the termini of the *N*-acetyllactosamine units extended from the GlcNAcβ1→6 branch of core 2 structures in human leukemic cell lines. On the other hand, we do not exclude the possibility that type 2 chains are extended from the Galβ1→3 residue of core 1 and/or the GlcNAcβ1→6 branch of I antigen structures as well as from the GlcNAcβ1→6 branch of core 2 structures. sLe^x epitopes may possibly be present on their termini and play an important role in collaboration with the same type of epitopes on the type 2 units from the core 2 backbones. However, proof of this requires further experiments.

For β1→4GalT expression, there was a discrepancy between the results using semiquantitative RT-PCR and immunoblot analyses. This would be due to a change of translational efficiency (36) or due to other possible β1→4GalT. However, further elucidation is required. The expression of C2GnT transcript and enzyme activity levels in TPA-treated KM3 cells were about 1/10 of those in control cells (Fig. 3, *B* and *C*, and Fig. 4). Despite the 1/10 down-regulation, cell surface sLe^x expression was not completely suppressed in flow cytometry analyses (Fig. 1*A*). This would be because the minimal level of C2GnT enzyme activities after TPA treatment was functionally enough to synthesize a certain (minimal) amount of sLe^x structures in